

Fig. 3 Schematic diagram of a transient flow pattern for a ring vortex-shock wave interaction: 1) shock wave, 2) primary sound wave, 3) secondary sound wave, 4) shear layer, and B) triple point.

the vortex; and 3) a toroidal wave (a sound wave) around the vortex core.

The normal shock wave is crossed by the toroidal wave (photograph 5). Since the radius of the vortex ring continuously increases, it remains larger than the radius of the jet. As a consequence, a part of the normal shock wave between the vortex core and the shear layer can move faster upstream owing to lower flow velocity in that region (arrow in photograph 6). This leads to shock-wave diffraction and eventually to the secondary sound-wave formation visible in photographs 7 and 8. Photograph 7 shows the stage when the toroidal wave has just reached the axes of the system. Now, the normal shock wave is accompanied by two sound waves: the primary (toroidal) wave and the secondary one. Both waves join at the triple point B (Fig. 3). The sound wave, after reflection at the axis of symmetry, spreads out in the surrounding space as a secondary sound pressure pulse (the primary one corresponds to the primary sound wave). It splits into two parts while it is passing through the vortex (photograph 9), analogous to the shock wave in the stage shown in photograph 4.

The photographs described above provide additional information on the flow under consideration. They show small vortices at the shear layer being sucked by a head vortex and in this way strengthening the head vortex. The sound-wave motion in the radial direction induces the shear layer instabilities, which are manifested in formation of discrete vortices (see photograph 9). However, the details of this process are difficult to explain on the basis of the photographs under discussion.

Conclusion

The vortex-shock wave interaction process in an axisymmetric flow leads to a complicated sound-wave pattern. It consists of the primary toroidal wave that appears as the shock wave passes through the ring vortex and a secondary wave that arises, with some delay, because of the strongly nonuniform flow velocity in the vortex plane. The primary wave diffracts while it crosses the ring vortex.

References

- ¹Pao, S. P., and Seiner, J. M., "Shock-Associated Noise in Supersonic Jets," *AIAA Journal*, Vol. 31, No. 5, 1993, pp. 687-693.
- ²Weeks, T. M., and Dosanjh, D. S., "Sound Generation by Shock-Vortex Interaction," *AIAA Journal*, Vol. 5, No. 4, 1967, pp. 660-669.
- ³Ribner, H. S., "Cylindrical Sound Wave Generation by Shock-Vortex Interaction," *AIAA Journal*, Vol. 23, No. 11, 1985, pp. 1708-1715.
- ⁴Pao, S. P., and Salas, M. D., "A Numerical Study of Two-Dimensional Shock-Vortex Interaction," *AIAA Paper* 81-1205, 1981.
- ⁵Kopriva, D. A., "A Multidomain Spectral Collocation Computation of the Sound Generated by a Shock-Vortex Interaction," *Computational Acoustics: Algorithms and Applications*, edited by D. Lee and M. Schultz, Vol. 2, Elsevier, Amsterdam, 1988.
- ⁶Meadows, K. R., Kumar, A., and Hussaini, M. Y., "Computational Study of the Interaction Between a Vortex and a Shock Wave," *AIAA Journal*, Vol. 29, No. 2, 1991, pp. 174-179.
- ⁷Dosanjh, D. S., and Weeks, T. M., "Interaction of a Starting Vortex as Well as a Vortex Street with a Traveling Shock Wave," *AIAA Journal*, Vol. 3, No. 2, 1965, pp. 216-223.
- ⁸Naumann, A., and Hermans, E., "On the Interaction Between a Shock Wave and a Vortex Field," *AGARD-CP-131*, 1973.

Boundary-Layer Transition Due to Isolated Three-Dimensional Roughness on Airfoil Leading Edge

M. J. Cummings* and M. B. Bragg[†]
University of Illinois at Urbana-Champaign,
Urbana, Illinois 61801-2935

Introduction

ICE roughness on an airfoil initially forms very near the leading edge in a region of favorable pressure gradient and rapidly grows to exceed the height of the boundary layer. Understanding the effect that hemispherical ice roughness has on the boundary-layer flow and heat transfer is a very important part of ice accretion physics. This investigation sought to answer two questions: 1) What is the critical-roughness Reynolds number for elements protruding out of the boundary layer and experiencing a pressure gradient and 2) how large is the transitional region behind a critical element?

Most classic experiments on roughness involved small roughness contained within a laminar boundary layer on a flat plate (no pressure gradient).¹⁻³ The roughness Reynolds number was defined as $Re_k = U_k k / \nu$, where k is the height of the roughness, ν the kinematic viscosity, and U_k the velocity of the undisturbed boundary-layer flow at the height of the roughness. The critical-roughness Reynolds number, $Re_{k,crit}$, was normally defined as the Re_k where transition occurred immediately behind the roughness element. Although a wide range of values for $Re_{k,crit}$ has been reported, a value of 600 generally has been accepted and used in practice for all roughness, particularly for fixing transition on wind tunnel models.⁴ In reality, transition does not occur at the element, but approaches the element asymptotically as Re_k is increased past the critical value.⁵

Braslow et al.⁴ and von Doenhoff and Horton⁶ noted an increase in $Re_{k,crit}$ for distributed roughness near the leading edge of an airfoil. $Re_{k,crit}$ values increased to approximately 1200 very near the leading edge, in part because of the pressure gradient and/or k/δ effects (δ is the undisturbed boundary-layer thickness). However, Smith and Clutter² as well as Peterson and Horton⁷ found little or no effect of pressure gradient alone. Peterson and Horton also reported no effect from varying k/δ for roughness within the boundary layer. However, Morkovin⁵ showed that for a fixed cylinder protruding out of the boundary layer, the flowfield instabilities that appear to lead to transition are different from those for the cylinder within the boundary layer. Presumably, this would alter the value of $Re_{k,crit}$, or possibly necessitate a new definition of $Re_{k,crit}$ for roughness protruding out of the boundary layer.

Thus, the motivation for the current study was to increase our understanding of $Re_{k,crit}$ and the transition region caused by large leading-edge roughness. The current investigation clearly revealed the inadequacy of assuming $Re_{k,crit} = 600$ near the airfoil leading edge. $Re_{k,crit}$ values in excess of 2000 were found, and the experiment suggests that even larger values may exist closer to the leading edge. The transition region behind the roughness extended well downstream before developing into a fully turbulent boundary layer and, in some instances, the transition region actually grew in length as Re_k (and, as a result, k/δ) was increased. This Note briefly describes these results. A more complete discussion of this research can be found in Cummings⁸ and Bragg et al.⁹

Received Sept. 1, 1995; revision received Nov. 6, 1995; accepted for publication Nov. 6, 1995. Copyright © 1996 by the American Institute of Aeronautics and Astronautics, Inc. All rights reserved.

*Graduate Research Assistant, Department of Aeronautical and Astronautical Engineering. Member AIAA.

[†]Professor, Department of Aeronautical and Astronautical Engineering. Associate Fellow AIAA.

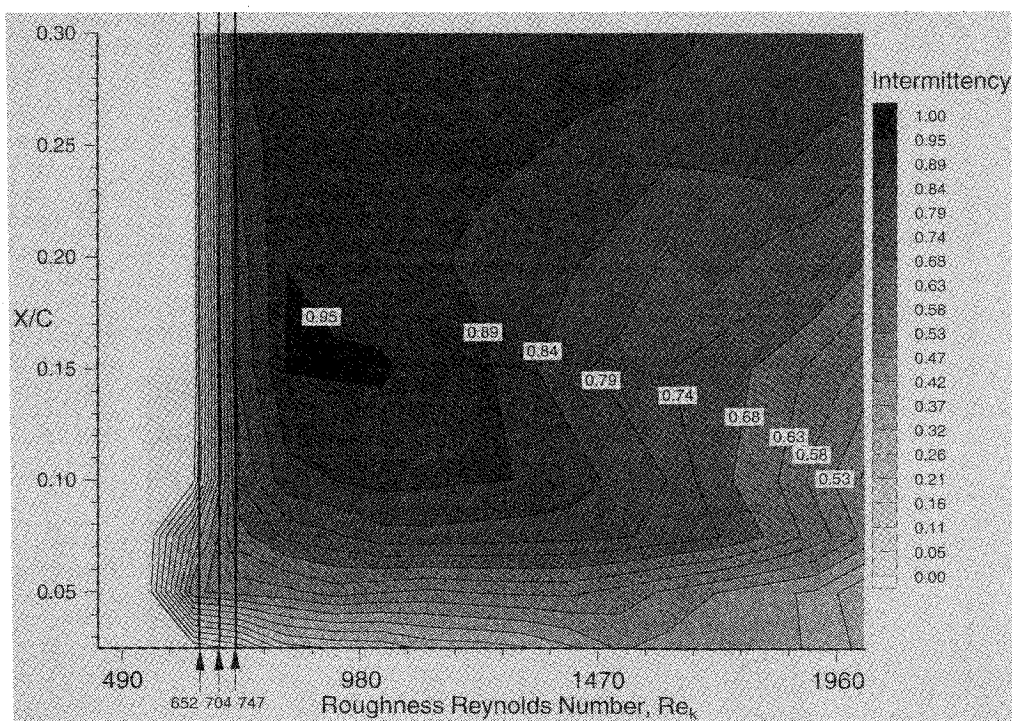


Fig. 1 Intermittency contours for varying Re_k due to a 0.5-mm high-roughness element at $x/c = 0.0163$ on a NACA 0012 airfoil at $\alpha = 0^\circ$ ($Re_k \pm 1.0\%$, $\alpha \pm 0.1^\circ$, and $x/c \pm 0.0005$).

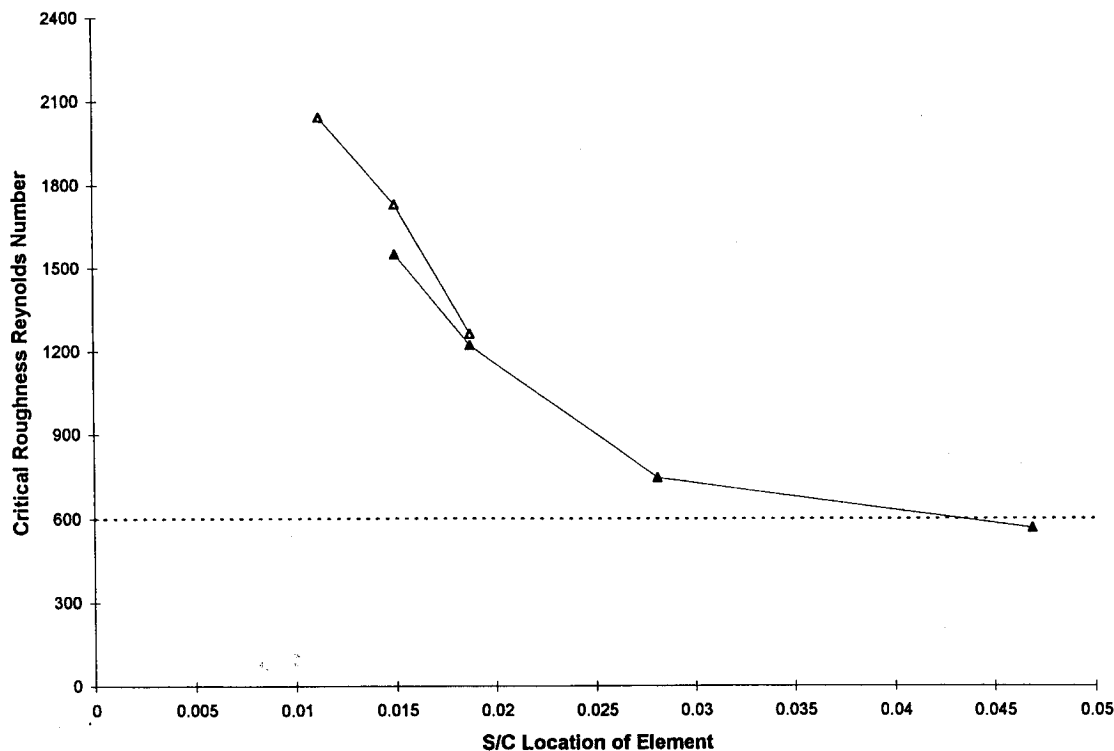


Fig. 2 Critical-roughness Reynolds number values as determined for the $I = 0.8$ criterion for various element locations and heights ($Re_{k,crit} \pm 1.0\%$ and $s/c \pm 0.0005$): \blacktriangle , 0.5-mm element; \triangle , 1.0-mm element; and ---, classic critical value.

Results and Discussion

The experiments were conducted in the 3×4 ft Low-Turbulence Subsonic Wind Tunnel at the University of Illinois at Urbana-Champaign⁸ where the turbulence intensity was $<0.1\%$. The model was a two-dimensional NACA 0012 airfoil with a chord of 533.4 mm (21 in.) at 0-deg angle of attack. Single 0.5- and 1.0-mm-high hemispheres were placed on the airfoil surface at 0-, 2-, 4-, 6-, 8-, 10-, 15-, and 25-mm surface lengths S from the leading edge ($x/c = 0.0, 0.0006, 0.0017, 0.0038, 0.0062, 0.0088, 0.0163$, and 0.0333 , respectively, where c is the airfoil chord length). The element heights

and locations were based on quantitative measurements of initial ice roughness accretions observed on a NACA 0012 airfoil.¹⁰

Measurements were made with a hot-wire probe placed at a constant height of 0.25-mm above the surface at several chordwise locations downstream of the element. For each measurement location, the model Reynolds number was increased from 0.45×10^6 to 2.05×10^6 in increments of 0.1×10^6 . At each increment, hot-wire data were recorded and reduced to give velocity, turbulence intensity, and intermittency. Intermittency is a measure of the amount of time the flow is turbulent. Laminar flow has an intermittency of 0.0,

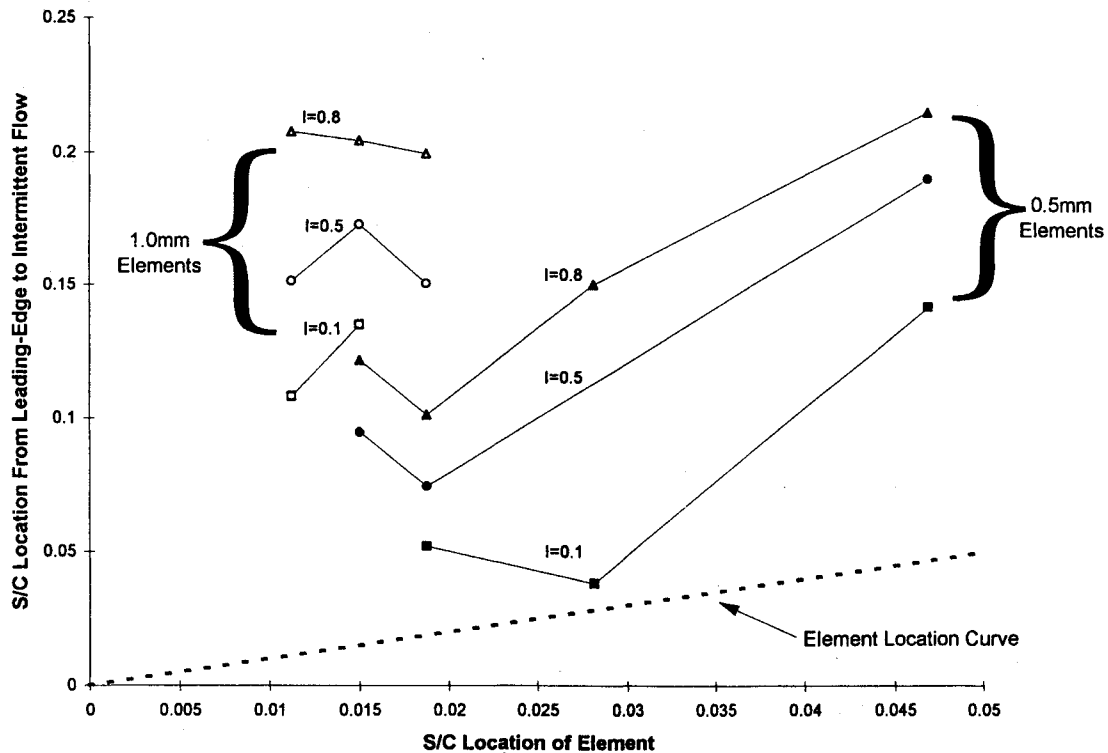


Fig. 3 Distance from leading edge to intermittent flow for various element locations and heights at $Re_{k,crit}$ ($s/c \pm 0.0005$ horizontal scale, ± 0.005 vertical scale).

whereas fully turbulent flow has an intermittency of 1.0. The intermittency method provided a better means of discerning turbulent flow than velocity or turbulence intensity alone.

A method similar to that of Tani et al.³ and Tani¹¹ was used to determine $Re_{k,crit}$ values. They recorded the transition Reynolds number Re_{tr} and the roughness Reynolds number Re_k at several chordwise locations downstream from the element, where transition was defined to be when intermittency reached 0.5 at a constant height above the surface. Transition Reynolds number was based on the freestream velocity and the surface length to the transition location. A linear fit of the data points, Re_{tr} vs Re_k , in the region of the rapid movement of transition toward the element was found and extended down to intersect with the limit curve where transition theoretically would have reached the element. This intersection determined $Re_{k,crit}$. Different values of intermittency can be used to reflect the different definitions used by different researchers for $Re_{k,crit}$.

Figure 1 shows the contours of intermittency obtained behind a 0.5-mm-high hemisphere located on the airfoil surface 15 mm behind the leading edge ($x/c = 0.0163$). This figure depicts the state of the boundary layer downstream of the roughness as the wind tunnel velocity was increased and therefore the model Reynolds number and roughness Re_k were increased, as shown on the horizontal scale. Note that near $Re_k = 700$, the roughness-induced transition region moved rapidly forward. The rapid movement of the transition process forward based on an $Re_{k,crit}$ criterion of $I = 0.1$ (as used by Klebanoff et al.¹), $I = 0.5$ (as used by Tani), and $I = 0.8$ (to model more closely the end of transition) are depicted as the heavy lines on the figure with the arrows depicting the extrapolated $Re_{k,crit}$ values. Note that at $Re_k = 700$, $k/\delta = 1.2$ for this element.

A summary of the $Re_{k,crit}$ values determined using the $I = 0.8$ criterion for the various hemisphere locations tested are presented in Fig. 2. The classic critical value of 600 is indicated by the dashed line for comparison. $Re_{k,crit}$ values determined with $I = 0.1$ and 0.5 were generally lower than the $I = 0.8$ criterion by only 5–19 and 1–9%, respectively, indicating rapid forward movement of transition. It is apparent that for hemispheres very near the leading edge ($x/c = 0.0038$, 0.0062, and 0.0088) where ice accretion typically occurs, the $Re_{k,crit}$ values are generally above 1000 and as high as 2000. In this region, k/δ values are typically 1.85–2.5 for the 0.5-mm elements and 2.4–4.9 for the 1.0-mm elements. Elements farther forward than $x/c = 0.0038$ did not cause premature transition

for the Reynolds numbers tested. It is anticipated that if the tunnel had been capable of higher speeds, $Re_{k,crit}$ values greater than 2000 would have been found in this region. As the elements were moved farther downstream from the leading edge, $Re_{k,crit}$ decreased and approached values near 600, particularly for the 0.5-mm hemisphere. Note that the 0.5-mm element at $x/c = 0.0333$ from the leading edge was within the boundary layer and the pressure gradient was mild so that it was not unexpected that the $Re_{k,crit}$ value was near the classic value of 600.

Recall that the hot-wire measurements were taken at a constant height of 0.25-mm off the surface to determine $Re_{k,crit}$. The height was chosen to capture the initial intermittency growth near the wall during the transition process. The location for the completion of transition cannot be completely defined by this method. To reliably determine this location, full boundary-layer velocity or intermittency profiles need to be taken.⁸ However, the near-wall intermittency recorded in the current test can be used as an indication of the development of transition. Figure 1 shows that while the roughness element initiated the transition process, the transition region extended well downstream. Here the element is at $x/c = 0.0163$, whereas an intermittency value of 0.9 near the wall approaches no closer than $x/c = 0.10$. Figure 3 compiles similar data for several of the roughness elements tested and shows the distance downstream where intermittency values of 0.1, 0.5, and 0.8 were found. These distances were taken at the $Re_{k,crit}$ value determined with the $I = 0.8$ criterion. Notice that the beginning of the transition process, as indicated by $I = 0.1$, occurred well downstream of the element with locations from $s/c = 0.03$ to 0.13. If $I = 0.8$ represented a location near the end of the transition process, this occurred from approximately $s/c = 0.1$ –0.20. Notice from Fig. 3 that the 1.0-mm elements caused transition farther downstream and, from Fig. 2, at larger values of $Re_{k,crit}$. This may be evidence of the effect of k/δ .

These distances, however, were taken only at a particular value of Re_k . If Re_k was increased beyond the critical value, the extent of the transition region could actually increase. From Fig. 1, $I = 0.8$ is reached in the boundary layer at approximately $x/c = 0.08$ for Re_k values just above the critical value. But as Re_k is increased, the distance to $I = 0.8$ increases dramatically past $Re_k = 1600$ where $k/\delta = 1.75$. Past this value of Re_k the entire transition region moves back downstream because the element was less effective in causing transition. This would appear to be a k/δ effect since increasing Re_k

for a given element size at a specific surface location occurred as the tunnel speed was increased and the boundary-layer thickness was reduced. Many of the elements tested exhibited this behavior, with the downstream movement of transition starting at higher Re_k and k/δ as the element location approached the leading edge.

Acknowledgment

This work was supported in part by Grant NAG 3-1134 from NASA Lewis Research Center.

References

- ¹Klebanoff, P. S., Schubauer, G. B., and Tidstrom, K. D., "Measurements of the Effect of Two-Dimensional and Three-Dimensional Roughness Elements on Boundary-Layer Transition," *Journal of the Aeronautical Sciences*, Vol. 22, No. 11, 1955, pp. 803, 804.
- ²Smith, A. M. O., and Clutter, D. W., "The Smallest Height of Roughness Capable of Affecting Boundary-Layer Transition," *Journal of the Aerospace Sciences*, Vol. 26, No. 4, 1959.
- ³Tani, I., Komoda, H., and Konatsu, Y., "Boundary-Layer Transition by Isolated Roughness," Rept. 375, Aeronautical Research Inst., Univ. of Tokyo, Japan, Nov. 1962.
- ⁴Braslow, A. L., Hicks, R. M., and Harris, R. V., "Use of Grit-Type Boundary-Layer-Transition Trips on Wind Tunnel Models," NASA TN D-3579, 1966.
- ⁵Morkovin, M. V., "Bypass Transition to Turbulence and Research Desiderata," NASA CP-2386, May 1984, pp. 161-204.
- ⁶Von Doenhoff, A. E., and Horton, E. A., "A Low-Speed Experimental Investigation of the Effect of a Sandpaper Type of Roughness on Boundary-Layer Transition," NACA Rept. 1349, 1956.
- ⁷Peterson, J. B., and Horton, E. A., "An Investigation of the Effect of a Highly Favorable Pressure Gradient on Boundary-Layer Transition as Caused by Various Types of Roughness on a 10-Foot-Diameter Hemisphere at Subsonic Speeds," NASA MEMO 2-8-59L, 1959.
- ⁸Cummings, M. J., "Airfoil Boundary-Layer Transition Due to Large Isolated 3-D Roughness Elements in a Favorable Pressure Gradient," M.S. Thesis, Univ. of Illinois at Urbana-Champaign, IL, 1995.
- ⁹Bragg, M. B., Kerho, M. F., and Cummings, M. J., "Airfoil Boundary Layer Due to Large Leading-Edge Roughness," AIAA Paper 95-0536, Jan. 1995.
- ¹⁰Shin, J., "Characteristics of Surface Roughness Associated with Leading Edge Ice Accretion," AIAA Paper 94-0799, Jan. 1994.
- ¹¹Tani, I., "Effect of Two-Dimensional and Isolated Roughness on Laminar Flow," *Boundary Layer and Flow Control*, edited by G. V. Lachmann, Vol. 2, Pergamon, Oxford, England, UK, 1961, pp. 637-656.

Pressure Fluctuations in an Unstable Confined Jet

Patricia Ern* and José Eduardo Wesfreid†

Ecole Supérieure de Physique et Chimie Industrielles,
75231 Paris Cedex 05, France

Introduction

THIS Note reports on a study of pressure fluctuations at the exit of a two-dimensional jet confined in a rectangular cavity. Experimental observations were made for various Reynolds numbers and cavity lengths. The results show an initial weak oscillation at lower Reynolds numbers followed by a strong self-sustained oscillation regime at higher Reynolds numbers, eventually perturbed by a noisy background. The main findings of this Note are an amplitude hysteresis between the frequency stages and a transition in the flow type behavior from convectively unstable to absolutely unstable. For a selection of related works, the reader is referred to Refs. 1-10.

Received March 11, 1995; revision received Oct. 20, 1995; accepted for publication Oct. 28, 1995. Copyright © 1996 by the American Institute of Aeronautics and Astronautics, Inc. All rights reserved.

*Boursière Docteur Ingénieur, Laboratoire Physique et Mécanique des Milieux Hétérogènes, URA CNRS 857, 10, rue Vauquelin.

†Directeur de Recherches, Laboratoire Physique et Mécanique des Milieux Hétérogènes, URA CNRS 857, 10, rue Vauquelin.

Experimental Setup

The experimental configuration composed a gravity-driven water flow discharging into the horizontal cavity. The cavity (Fig. 1) was a parallelepipedic chamber 10 cm wide and 2.5 cm high. Its length L was selected by moving the right-hand end wall. At the middle height of the cavity, the jet had a uniform velocity profile over about 70% of its width. The Reynolds number Re was based on the inflow characteristics at the point of the expansion, i.e., nozzle width of 0.4 cm, mean velocity U_m obtained as the flow rate divided by a nozzle section $2.5 \times 0.4 \text{ cm}^2$, and a dynamic viscosity of $1.05 \times 10^{-3} \text{ Pa} \cdot \text{s}$. The flow rate was regulated with two precision needle valve rotameters, placed after the jet chamber to avoid perturbations in the flow. Two rotameters, Vögtlin V100-300 09 and V100-300 12, of 1% accuracy were used. Errors in viscosity and velocity induced an error of approximately 5% on the Reynolds number.

A variable reluctance pressure transducer Validyne type DP-103-10-N1S4D was used. The detecting holes were placed at half of the height of the cavity and 0.2 cm away from the exit contraction corner, as shown in Fig. 1. The transducer was associated with a Validyne CD15 carrier demodulator (1-V output signal for 8.63-Pa differential pressure). This signal was sent to a Fourier analyzer Scientific-Atlanta SD380. The flow rate was varied in steps of $0.28 \text{ cm}^3/\text{s}$, in either increasing or decreasing sequences. At each step, once the flow was stabilized, 500 pressure-spectra samples were averaged. Visualization of the flow was performed simultaneously by injecting fluorescein dye. Results will be discussed for $L = 5 \text{ cm}$ and $L = 7 \text{ cm}$, but for brevity, only the experiments for $L = 7 \text{ cm}$ will be shown in the figures.

Results and Discussion

Spectra Analysis and Nature of the Oscillations

Figure 2 shows several pressure spectra observed for $L = 7 \text{ cm}$ at different Reynolds numbers. For the longer cavities studied ($L \geq 6 \text{ cm}$), the jet oscillation started at small flow rates ($Re \sim 160$) with a low-frequency f_L lying in the $\sim 0.3\text{--}0.4 \text{ Hz}$ range. The oscillation at this frequency had a small amplitude, and the spectrum also contained harmonics, notably, $2f_L$. As the Reynolds number was increased, these peaks grew and broadened. This broad spectrum is characteristic of a convective instability in open flows.¹¹ For a specific flow rate ($Re \sim 210$) that depended on the cavity length the spectrum suddenly concentrated on one sharp peak f_1 of a considerably higher amplitude. It seemed that the feedback was then synchronized with the instability wave, thus corresponding to self-sustained oscillating behavior.¹² Such an abrupt change in the peak width is similar to that observed by Babcock et al.¹³ for a Taylor-Couette experiment with an axial flow.

In previous studies just using visualization methods,^{14,15} it was shown that only time-periodic discrete frequencies could be observed and could be associated with different integer modes n , scaling L to the wavelength λ according to the well-known Brown-Curle¹⁶⁻¹⁸ phenomenological relation^{2,3} $\lambda = L/(n + \frac{1}{4})$. In Fig. 2, the intense peak at frequency f_1 for $Re \sim 210$ corresponds to the wavelength of mode $n = 3$ for $L = 7 \text{ cm}$ ($n = 2$ for $L = 5 \text{ cm}$). As the Reynolds number was increased, the frequency f_1 increased

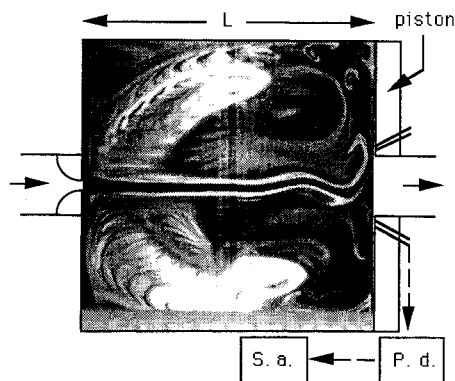


Fig. 1 Cavity geometry and differential pressure detection: pressure detector (P.d.) and spectrum analyzer (S.a.).